Simulation-Based Coyote Optimization Algorithm to Determine Gains of PI Controller for Enhancing the Performance of Solar PV Water-Pumping System

Jouda Arfaoui [1], Hegazy Rezk [2,3,*], Mujahed Al-Dhaifallah [4,*], Mohamed N. Ibrahim [5,6,7] and Mami Abdelkader [8]

[1] National School of Engineering of Tunis, University of Tunis ELMANAR, BP 37, Tunis 1002, Tunisia; jouda.arfaoui@gmail.com
[2] College of Engineering at Wadi Addawaser, Prince Sattam Bin Abdulaziz University, Al-Kharj 11991, Saudi Arabia
[3] Electrical Engineering Deprtment, Faculty of Engineering, Minia University, Al Minya 61519, Egypt
[4] Systems Engineering Department, King Fahd University of Petroleum & Minerals, Dhahran 31261, Saudi Arabia
[5] Department of Electromechanical, Systems and Metal Engineering, Ghent University, 9000 Ghent, Belgium; m.nabil@ugent.be
[6] FlandersMake@UGent—Corelab EEDT-MP, 3001 Leuven, Belgium
[7] Electrical Engineering Department, Kafrelshiekh University, Kafr el-Sheikh 33511, Egypt
[8] Department of Physics, Faculty of Sciences, University Tunis El Manar, BP 37, Tunis 1002, Tunisia; abdelkader.mami@gmail.com
* Correspondence: hr.hussien@psau.edu.sa (H.R.); mujahed@kfupm.edu.sa (M.A.-D.)

check for updates

Abstract: In this study, a simulation-based coyote optimization algorithm (COA) to identify the gains of PI to ameliorate the water-pumping system performance fed from the photovoltaic system is presented. The aim is to develop a stand-alone water-pumping system powered by solar energy, i.e., without the need of electric power from the utility grid. The voltage of the DC bus was adopted as a good candidate to guarantee the extraction of the maximum power under partial shading conditions. In such a system, two proportional-integral (PI) controllers, at least, are necessary. The adjustment of (Proportional-Integral) controllers are always carried out by classical and tiresome trials and errors techniques which becomes a hard task and time-consuming. In order to overcome this problem, an optimization problem was reformulated and modeled under functional time-domain constraints, aiming at tuning these decision variables. For achieving the desired operational characteristics of the PV water-pumping system for both rotor speed and DC-link voltage, simultaneously, the proposed COA algorithm is adopted. It is carried out through resolving a multiobjective optimization problem employing the weighted-sum technique. Inspired on the *Canis latrans* species, the COA algorithm is successfully investigated to resolve such a problem by taking into account some constraints in terms of time-domain performance as well as producing the maximum power from the photovoltaic generation system. To assess the efficiency of the suggested COA method, the classical Ziegler–Nichols and trial–error tuning methods for the DC-link voltage and rotor speed dynamics, were compared. The main outcomes ensured the effectiveness and superiority of the COA algorithm. Compared to the other reported techniques, it is superior in terms of convergence rapidity and solution qualities.

Keywords: simulation-based optimization; coyote optimization algorithm; water pumping; energy efficiency

1. Introduction

Thanks to the huge availability of the sun supply in comparison with other energy sources, the solar PV systems seem one of the most encouraging applications of renewable energy today and in the forthcoming years. Moreover, the cost of the PV modules is reducing increasing a result of the progress in the manufacturing technology of the solar modules [1]. Standalone and grid-connected systems are the two main types of solar systems. Indeed, Sun availability is taking as one of the most important motivation for depending on the solar system as a promising solution. As being a type of renewable energy resources, the solar PV has gained a growing importance for uses in the electric power domain which has several advantages like (1) being harmless energy, (2) being suitable for isolated sites and (3) being cheap and easy maintenance.

Indeed, the efficiency and cost of the PV pumping system are not attractive yet to spread widely, but, many literature works are devoted to improving the total effectiveness and reducing the total cost of the solar pumping generation system [1,2].

A major drawback of using this sort of vector control lies in the fact that the effectiveness of the water-pumping system is in the heavy dependence on the appropriate adjustment of the PI parameters. Commonly, the set of these parameters is based on the classical and tiresome trials and error methods [3–6].

Adjustment method turned out to be complex and time-consuming. Moreover, the conventional PI tuning approach such as the symmetrical optimum [7], Ziegler–Nichols [8], Tyreus–Luyben [9] and Cohen–Coon [10] techniques requires that the designer has a good insight about the characteristics and dynamics of the controlled system. Hence, for the sake of overcoming these drawbacks, a systematic process to identify best gains of PI regulators has been provided in [3] and the modern optimization is considered as an auspicious solution.

In [11] the authors considered two optimization metaheuristics: Ant colony optimization (ACO) and differential evolution (DE). These strategies are reported to provide an optimized adjustment (PI) regulators in the direct torque control–space vector modulation (DTC-SVM) control loops, like rotor speed, electromagnetic torque, stator flux linkage and estimation of the linkage stator flux. Compared to other metaheuristics methods, those considered approaches require few tuning parameters to provide a fast convergence rate. Simulation and practical experimental on three phase induction motor (TIM) controlled by DTC-SVM are carried out. On the other hand, classical procedures such as frequency and root locus have been applied.

In [12], the study reported a novel optimization algorithm that combines all these three techniques: genetic algorithm (GA), artificial neural networks (ANN) and fuzzy logic, which was named as GNFPID. This technique aims to outperform the performance of the used PID controller. In [13], a genetic algorithm is applied as the adequate adjustment method of PI controllers applied to DTC drive for doubly fed asynchronous machine. Following in the same strategy, particle-swarm optimization (PSO), bat algorithm (BA) and genetic algorithm (GA) are considered for the adequate tuning of the gains of PI for brushless DC motor in [14].

Metaheuristics are an iterative processes for solving different optimization problems by taking into account simple trial operations [15,16]. Particle-swarm optimization [17], genetic algorithm [18], Imperialist competitive algorithm [19], ant colony optimization [20,21], differential evolution [22,23] are commonly treated. In [24], water cycle algorithm was adopted to adjust the parameters of PI controller for speed control and reactive power control loops in RSC (rotor side converter) and DC-link regulation voltage loop in GSC (grid side converter).

In the same way, [25] has referred to a thermal exchange optimization (TEO), this metaheuristic method was applied for the tuning of PI controller gains for the external loops in the conventional vector control strategy of a doubly fed induction generator based on wind turbine system. For assessing the efficiency and superiority of the proposed control strategy, other well-known metaheuristic procedures such as grasshopper optimization algorithm (GOA), particle-swarm optimization (PSO),

water cycle algorithm (WCA) and harmony search algorithm (HSA), are taken into account for comparison purposes.

To best of our knowledge, for first time, the coyote optimization (COA) algorithm is used to identify the parameters of PI controller to improve the performance of solar PV water-pumping system under partial shading condition. Therefore, in this study, COA algorithm is investigated and further, to prove the superiority of the suggested COA algorithm, the obtained results are compared with the classical Ziegler–Nichols method, trial–error tuning method and PSO algorithm.

The remainder of this study is arranged as follows: the mathematical model of the solar photovoltaic water-pumping system (SPWPS) is described in Section 2. Section 3 is devoted to the formulation of the outer-loops PI controllers' design problem given as a constrained optimization problem. The proposed COA method is given in detail, aimed to resolve such a problem. In Section 4, the demonstrative results of the COA-tuned PI controllers tuning are carried out. Concluding remarks are summarized in Section 5.

2. Modeling of the Solar Photovoltaic Water-Pumping System

Referring to the solar pumping system, several control methods were developed to provide an effective functioning. These include speed control, distinct maximum power point tracking (MPPT) techniques, voltage control and frequency regulation under load variation [26].

This part studies and simulates a new structure of a solar pumping system. The overall structure of the proposed PV pumping system is described, as well as its various subsystems.

Vector control also called field-oriented control, is a method that permits independent control of the flux and torque components. It is equipped with high-performance drives. In this section, the interest is focused on the type of control.

The proposed system includes the following parts: PV panel, three-phase voltage inverter, DC–DC boost converter and induction engine-driven pump unit.

A schematic diagram of the new structure including indirect field oriented control (IFOC) and MPPT strategies, is illustrated in Figure 1. Concerning the control of this sort of system, different techniques were considered for effective functioning in terms of speed control, voltage control, distinct MPPT techniques and frequency regulation under load variations. The most important parts of this system are indicated in Figure 1 and are recapitulated as follows:

(1) Shaded PV modules represent the power supply source of the induction engine via a three-phase voltage source inverter (VSI);

(2) A hysteresis pulse-width modulation (PWM) based current control;

(3) A boost converter for forcing the PV panel to operate at the MPP under different partial shading conditions [27];

(4) Flux weakening component is required to produce the reference current (I_{ds}^*) and the speed controller output gives (I_{qs}^*);

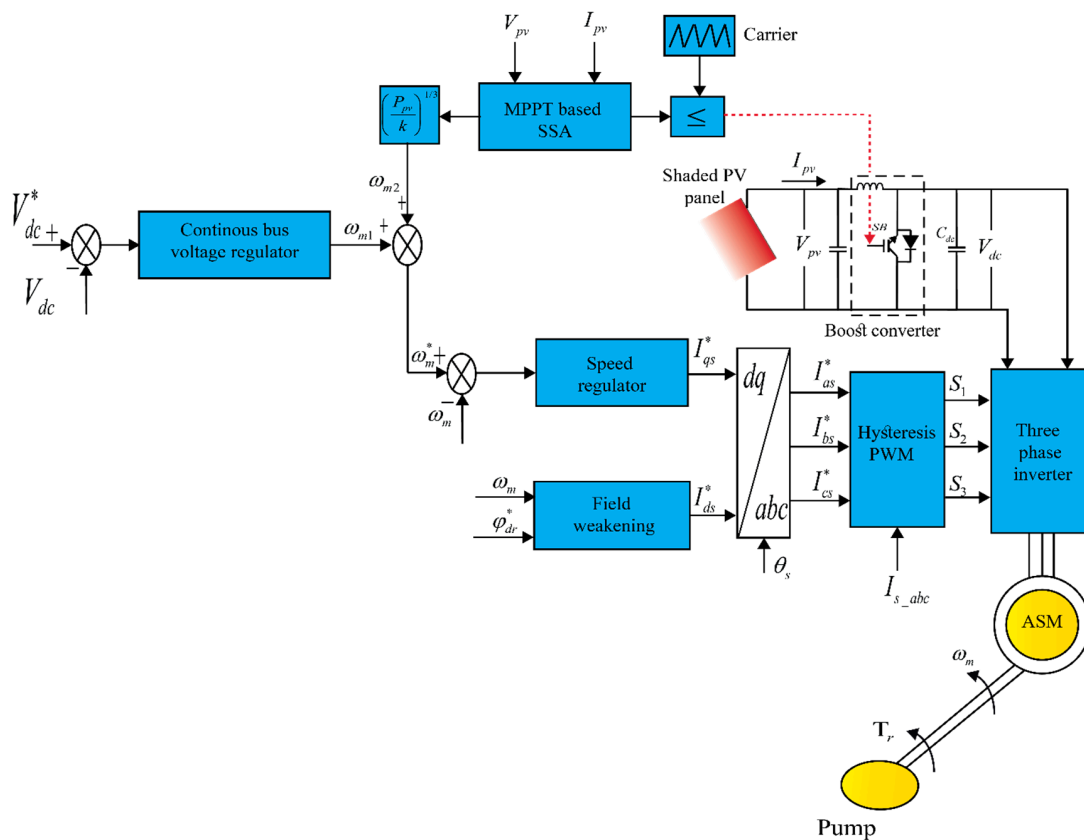(5) Vector control of asynchronous machine for driving centrifugal pump [28].

Figure 1. Scheme diagram of the proposed system.

The reference speed is a measure of the generated PV power. The PI controllers' design and the suitable values of the gains regulators (K_{ps}, K_{is}, K_{pdc} and K_{idc}) are typically tuned employing trials and errors technique, as mentioned before. Regarding the control design stage of VSI, this hard and challenging task turns into more difficult and time-consuming. A recent global meta-heuristic algorithm is an effective solution to tackle this matter.

2.1. Model of the Induction Machine

In this context, the Park transformation is adopted when modeling the asynchronous machine to omit the inductance variation with time [29].

$$V_{ds} = R_s I_{ds} + \sigma L_s \frac{dI_{ds}}{dt} + \frac{L_m}{L_r} \frac{d\varphi_{dr}}{dt} - \omega_s \sigma L_s I_{qs} \tag{1}$$

$$V_{qs} = R_s I_{qs} + \sigma L_s \frac{dI_{qs}}{dt} + \omega_s \frac{L_m}{L_r} \varphi_{dr} + \omega_s \sigma L_s I_{ds} \tag{2}$$

$$V_{dr} = 0 = \frac{R_r}{L_r} \varphi_{dr} + \frac{d\varphi_{dr}}{dt} - \frac{L_m}{L_r} R_r I_{ds} \tag{3}$$

$$V_{qr} = 0 = \omega_{sl} \varphi_{dr} - \frac{L_m}{L_r} R_r I_{qs} \tag{4}$$

where

$$\sigma = 1 - \frac{L_m{}^2}{L_s L_r}$$

V_{ds}, V_{qs}, V_{dr} and V_{qr} indicate the stator and the rotor voltages, respectively.

I_{ds} and I_{qs} represent the stator currents.

$$\varphi_{dr} = L_m I_{mdr} \tag{5}$$

$$I_{ds} = I_{mdr} + \frac{L_r}{R_r} \frac{dI_{mdr}}{dt} \tag{6}$$

$$I_{ds} = (1 + p \cdot \tau_r) I_{mdr} \tag{7}$$

where

$$\tau_r = \frac{L_r}{R_r}$$

In steady states conditions

$$I_{ds} = I_{mdr} \tag{8}$$

The instantaneous value of the angle θ_s is determined by this equation:

$$\theta_s = \int \omega_s dt \tag{9}$$

$$\theta_s = \int \omega_s dt = \int (\omega_{sl} + \omega_r) dt \tag{10}$$

The sliding speed ω_{sl} can be calculated using this equation [29]:

$$\omega_{sl} = \frac{L_m}{L_r} \frac{R_r}{\varphi_{dr}} I_{qs} = \frac{L_m I_{qs}}{\tau_r \varphi_{dr}} = \frac{I_{qs}}{\tau_r I_{mdr}} \tag{11}$$

In steady states conditions ($I_{mdr} = I_{ds}$) and thus

$$\omega_{sl} = \frac{I_{qs}}{\tau_r I_{ds}} \tag{12}$$

Equations (13) and (14) are needed to determine the reference flux and reference stator current, respectively [29]:

$$\varphi_{dr}^* = \begin{cases} \varphi_{rn} & si \ |\omega_m| \leq \omega_{mn} \\ \frac{\varphi_{rn}\omega_{mn}}{|\omega_m|} & si \ |\omega_m| > \omega_{mn} \end{cases} \tag{13}$$

where φ_{rn} denotes nominal value of flux.

ω_{mn} denotes nominal value of mechanical speed

$$I_{ds}^* = \frac{\varphi_{dr}^*}{L_m} \tag{14}$$

L_m: is the mutual inductance

$$I_{qs}^* = T_e^* / \frac{3}{2} \frac{P L_m}{2 L_r} \varphi_{dr}^* \tag{15}$$

The correlation process between the torque and the speed of the pump model is described as follows [30]:

$$T_r = a_1 + a_2 \cdot \omega_m^2 \tag{16}$$

where

a_1: constant;
a_2: constant;
T_r: Torque of pump;
w_m: motor speed.

The power of the pump has a cubic relationship with the motor speed w_m, thus driving the centrifugal pumps [31,32].

To evaluate one of the reference speed components, an affinity law shall be applied for this purpose. Under different solar irradiation, the induction machine operates and seeks to determine the centrifugal pump flow rates. Moreover, to optimize the produced PV power, a MPPT control was investigated. It enables the extraction of the global MPP. The generated power serves to determine the first component of the reference speed as follows [33]:

$$\omega_{m1} = \left(\frac{P_{pv}}{k}\right)^{1/3} \tag{17}$$

The PV array power is converted in terms of speed via the constant k.

The second component of the reference speed is evaluated by means of the DC-link voltage controller. In this system, a comparison between the measured bus voltage (V_{dc}) and the desired bus voltage (V_{dc}^*), is carried out, which conducts to a voltage error (ΔV_{dc}), described as [34]:

$$\Delta V_{dc}(n) = V_{dc}^*(n) - V_{dc}(n) \tag{18}$$

The output speed can be obtained by the following equation [34]:

$$\omega_{m2}(n) = \omega_{m2}(n-1) + K_{pdc}\{\Delta V_{dc}(n) - \Delta V_{dc}(n-1)\} + K_{idc}\cdot\Delta V_{dc}(n)\} \tag{19}$$

where K_{pdc} and K_{idc} are, respectively the proportional and integral parameters of the DC-link-voltage controller.

The reference speed of the induction motor is obtained according to the following equation [33]:

$$\omega_m^* = \omega_{m1} + \omega_{m2} \tag{20}$$

where ω_m^* is the reference speed and w_{m1} is the first part of reference speed, determined by means of Equation (17).

w_{m2} is the second part of reference speed, determined by means of Equation (19).

2.2. Pump Model

The mechanical model of the induction motor actuating the centrifugal pump is provided by the following formula [35]:

$$T_e - T_r - f\omega_m = J\frac{d\omega_m}{dt} \tag{21}$$

T_r and T_e represent the load torque and the electromagnetic torque, respectively, J is the moment of inertia and f is the damping coefficient which links the friction torque C_f to the motor speed by relation ($C_f = -f\omega_m$).

The following equation used to represent the pump torque [33]:

$$T_r = A_p\omega_m^2 \tag{22}$$

where A_p denotes torque constant and estimates as following [33]:

$$A_p = \frac{P_n}{\omega_{mn}^3} \tag{23}$$

where P_n and w_{mn} indicate rated power and nominal value of mechanical speed, respectively.

2.3. Three-Phase Voltage Inverter

To achieve an optimum control of the power supply between the PV source and the asynchronous engine, a voltage source inverter is required as a crucial part. The employed inverter consists of three independent arms, as illustrated in Figure 2. DC–AC converters are dealing with in this section, which already applied in the solar energy sector as well as in the three-phase voltage inverters. The state of the switches (k_n) has a considerable impact on the inverter modeling. The produced voltages are provided by the following matrix form [36]:

$$\begin{bmatrix} V_1 \\ V_2 \\ V_3 \end{bmatrix} = \frac{V_{pv}}{3} \begin{bmatrix} 2 & -1 & -1 \\ -1 & 2 & -1 \\ -1 & -1 & 2 \end{bmatrix} \begin{bmatrix} S_1 \\ S_2 \\ S_3 \end{bmatrix} \tag{24}$$
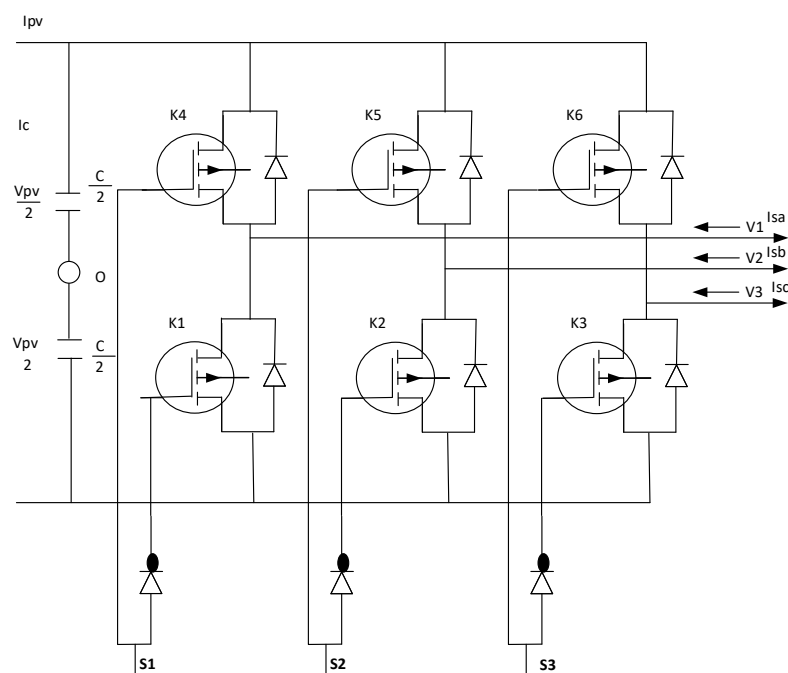
Figure 2. Three-phase voltage inverter.

The current provided by the DC source obeys to;

$$I_{pv} = S_1 I_{sa} + S_2 I_{sb} + S_3 I_{sc} + I_c \tag{25}$$

A PWM hysteresis strategy is employed to control these power converters.

2.4. DC–DC Boost Converter

An ideal scheme of the DC–DC boost converter is illustrated in Figure 3. The relation of proportionality between the input voltage (E) and the output voltage, is described as follows:

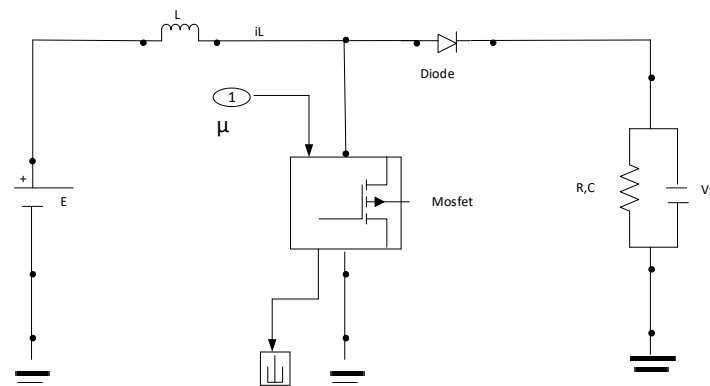$$V_s = \frac{E}{1 - u} \tag{26}$$

where u denotes the duty cycle.

Figure 3. Scheme of DC converter.

The DC converter can be integrated with MPPT strategy to extract the maximum power from the PV array.

2.5. Hysteresis Based PWM Current Controller

In most studies, the PWM technique is the most common strategy since it perfectly adapts with the use of the voltage inverter. It is recommended also in case the vector control is adopted.

The principle of this command as presented in Figure 4 is to generate a PWM signal based directly on the variable to be controlled, through decisions based on the on–off control. In addition, it consists of maintaining the variation of the measuring currents within a band at a self-adjusting width, centered on the reference currents. The hysteresis comparator of any PWM structure receives as an input signal: the difference between the reference and measurement currents in order to produce at the output the control signal for the power switches [36]. In fact, this control is simple to operate as it does not require precise knowledge of the machine but suffers from the lack of control of the switching frequency.
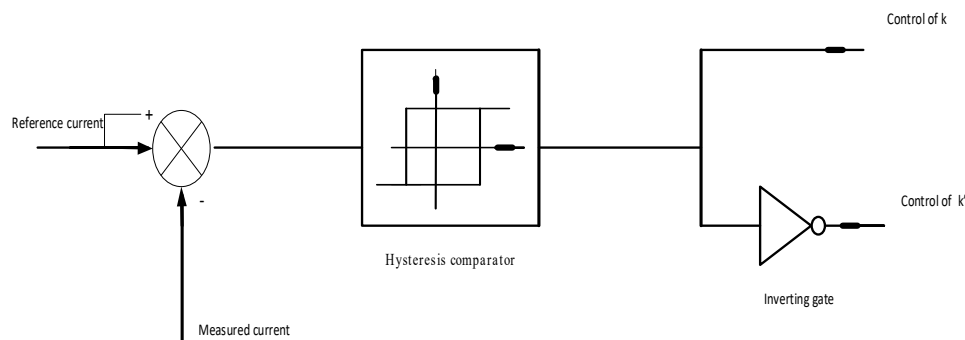

Figure 4. Schematic diagram of the hysteresis pulse-width modulation (PWM) control.

3. COA Design for Optimal PI Parameters Tuning

The coyote optimization algorithm (COA) was recently proposed by Pierezan and Coelho [37]. The core idea of COA optimizer is based on *Canis latrans* species that reside mainly North America [37]. The algorithm is adapted to consider the social organization of the agents called coyotes and it has been serving with a different algorithmic construction. The greatest advantage of this method is to preserve a balance between the exploitation and exploration mechanisms during that optimizing process. By contrast with the gray wolf optimization (GWO), the COA does not center on how these dominant norms have been followed by these animals and the social hierarchy. Additionally, the COA depends not only on the hunting preys which take place in the GWO, but also on the social structure and regular experience interchange which are carried out by the coyotes. They are distinguished by cooperative functionalities as they head toward the prey in the close chain while they have a strong

sense of smell which makes it possible to identify the location of the prey. Regarding the hunting process, coyotes attack in groups, this action forces the agents to update their positions to improve them. When coyotes' striking their opponents, they are well-prepared with a probability of threat and move away from their current position by an excessive random distance. Further, the COA method is initialized by an initializing population of coyotes whose size can be defined as the multiplication of packs and coyotes. The number of agents called coyotes in each pack is supposed to be equal and constant. In that regard, to facilitate the users' understanding, each coyote can be considered as a candidate solution for the optimization problem and its social condition presents the fitness function. The COA optimization algorithm started by a population of coyotes that are created randomly within the search space. More details about physical meaning and mathematical representation can be found in Ref [37,38]. Figure 5 presents the optimization process of COA.
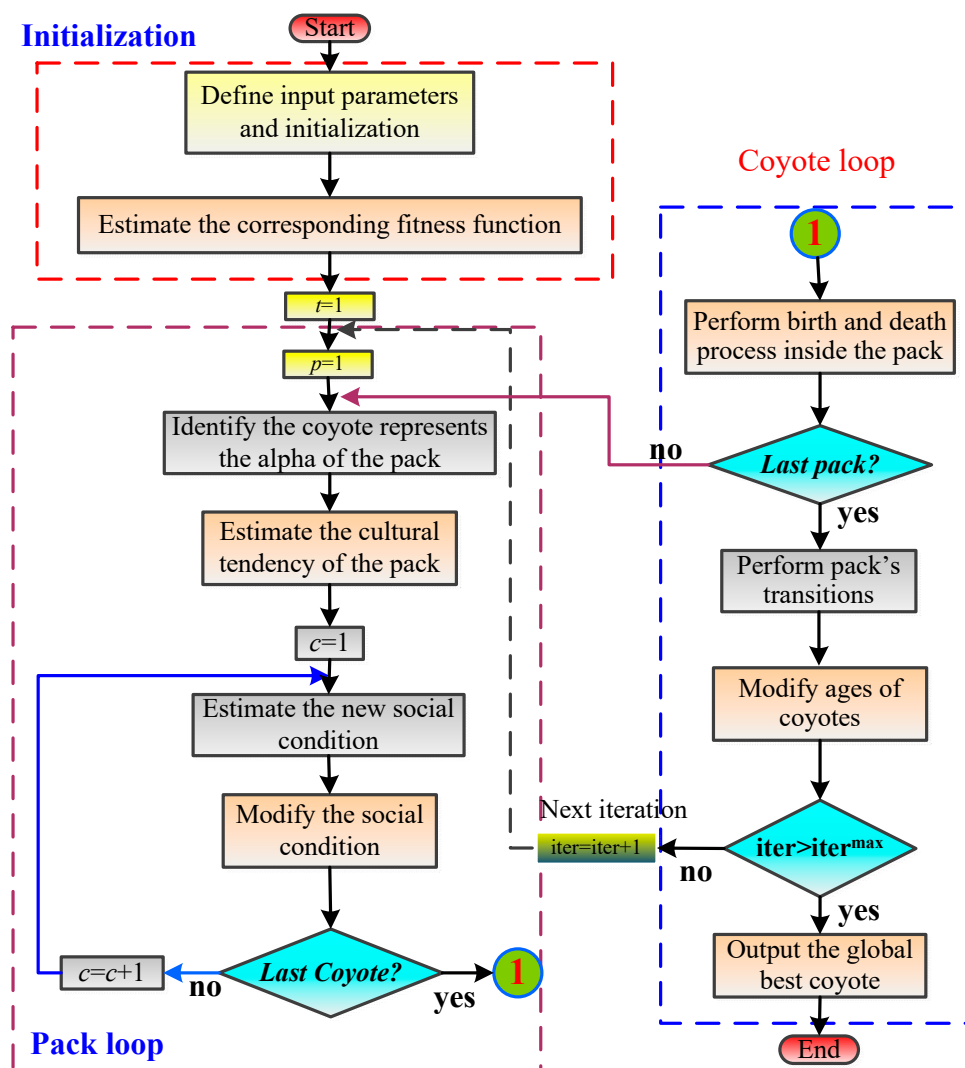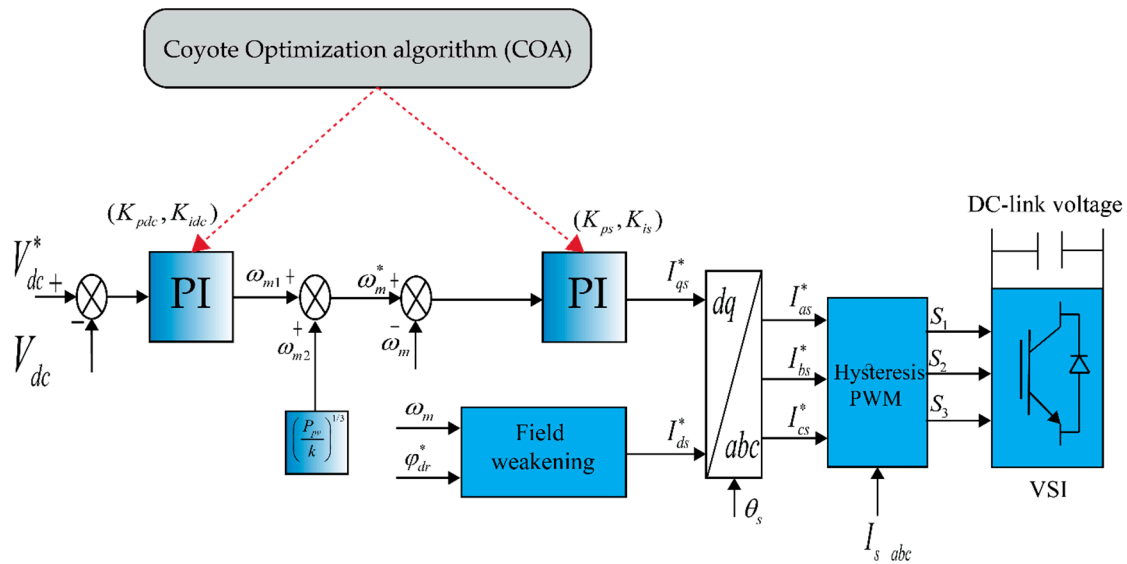

Figure 5. Optimization process of coyote optimization algorithm (COA).

Regarding the PI design control, the suitable parameters of this type of controllers are usually tuned by trials and error techniques [3–6]. This non-systematic process turns into more complicated and into more time-consuming, particularly for the complex systems' design. Accordingly, the idea of transforming the identification process of these parameters (K_{ps}, K_{is}, K_{pdc} and K_{idc}) to an optimization problem, is a promising alternative. By means of some advanced meta-heuristic algorithms, such optimization problems can be effectively managed [3]. Within the framework

provided, two interactive PI regulators for speed and DC-link voltage loops are being introduced. These PI regulators are demanded to achieve an optimized value of this control using such COA algorithm. Figure 6 provides the suggested tuning process of PI controllers for the solar photovoltaic water-pumping system (SPVWPS) based on optimization approach.

Figure 6. Proposed metaheuristics-tuned proportional-integral (PI) controllers for the solar photovoltaic water-pumping system (SPVWPS).

During the optimization process, the gains of PI controllers for the DC-link voltage and speed loops are considered as the decision variables of the problem, these parameters are denoted as follows:

$$x = \left[K_{pdc}, K_{idc}, K_{ps}, K_{is}\right]^T \in \mathbb{S} \subseteq \mathbb{R}^4_+ \tag{27}$$

where K_{pdc} and K_{idc} indicate the proportional and integral gains of DC-link regulator and K_{ps} and K_{is} denote the proportional and integral gains of speed regulator.

Under time-domain, such constraints like rise time, maximum overshoot, settling time and steady-state error of the system step-response, the performance criterion is minimized according to the suitable parameters of the problem [3].

The tuning process based on optimization is defined as follows:

$$\begin{cases} \text{minimize } g_i(x) \\ x = \left[K_{pdc}, K_{idc}, K_{ps}, K_{is}\right]^T \in \mathbb{S} \subseteq \mathbb{R}^4_+ \\ \text{subject to : } \\ h_1(x) = \delta_{Vdc} - \delta_{Vdc}^{max} \leq 0 \\ h_2(x) = \delta_{speed} - \delta_{speed}^{max} \leq 0 \end{cases} \tag{28}$$

In formulating the optimization problem, cost function are outlined as follows:

$$g_{IAE,i}(x) = \int\limits_0^\infty \left|e_i(x,t)\right| dt \tag{29}$$

Which are adopted the Integral of Absolute error (IAE) and maximum overshoot (MO) criteria, $\mathbb{S} = \left\{x \in \mathbb{R}^4_+, x_{low} \leq x \leq x_{up}\right\}$ is the initial search space.

Under such circumstances and to show superior performance, some constraints had to be considered in the optimization framework, $h_j : \mathbb{R}^4_+ \to \mathbb{R}, j \in \{1, 2\}$ presented the inequality constraints which are considered for this optimization process.

The terms δ_{dc} and δ_{speed} are the overshoot of the DC-link voltage and rotor speed, respectively. The optimization process described in Equation (28) is considered as a multi-objective optimization type; an aggregate of all costs functions to form one single objective function is determined by means of an aggregation function [3].

$$g(x) = \sum_{i=1}^{2} \omega_i g_i(x) \tag{30}$$

where $w_i > 0$, it denotes the weighting coefficients of the aggregation cost function. The objective function befitting for COA-tuned PI regulators for SPVWPS under shading condition, reformulated as follows:

$$g(x) = \int_0^{+\infty} (\omega_1 |w_r^* - w_r| + \omega_2 |v_{dc}^* - v_{dc}|) dt \tag{31}$$

4. Results and Discussion

The considered system in this research work contains a three-phase induction motor drive of 2200 W, 230 V, used to feed the water-pumping system. The main source is PV array with rating of 2400 W. The PV array composed of 234 PV module. The number of series PV modules interconnected is series is 18 modules whereas number of parallel string is 13 strings. The open circuit voltage and short circuit current of PV modules are 21.6 V and 0.64 A, respectively whereas the voltage and current at maximum power point are 17.6 V and 0.58 A. The case study considered the partial shading condition, three different level of the solar radiation; 1.0 kW/m^2, 0.8 kW/m^2 and 0.5 kW/m^2 are subjected to the PV array.

In order to tackle the problem of time-consuming, the PI control tune by COA is performed, which further highlights the contribution of the proposed adjustment approach based on metaheuristic versus the given classical Ziegler–Nichols and Trial and Error method.

Table 1 provides a summary of the obtained gains of the PI controllers for the classical based methods and the proposed optimization meta-heuristic called the coyote optimization algorithm (COA). Furthermore, a comparison is carried out between the obtained results for the proposed COA-tuned PI controllers and those obtained by the well-known Ziegler–Nichols and Trial and Error method for the PI controllers' design of DC-link voltage (Table 2 and Figure 7).

Table 1. Optimized PI controller gains.

Parameter	Algorithms		
	Trial and Error	**Ziegler–Nichols**	**COA**
K_{ps}	0.2499	4.78577	1.8706
K_{is}	16.9730	229.6941	3.8149
K_{pdc}	1	0.3052	2.7748
K_{idc}	500	62.2047	1.3374

Table 2. Output performance under different methods.

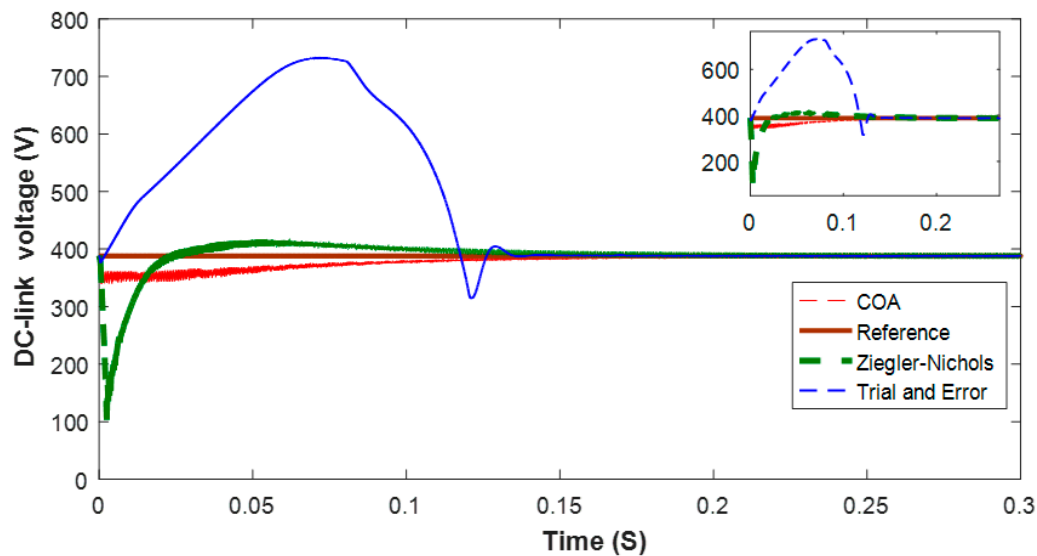| Methods	δ (%)	tr (sec)	ts (sec)	Ess
Trial–Error	20	0.1238	0.26	0.006
Ziegler–Nichols	5.1	0.0279	0.2	0.004
PSO-Method	0	0.0332	0.987	0.03
COA-Method	0	0.015	0.151	0.001

Figure 7. DC-link voltage under different methods.

According to these results, COA-tuned PI controllers with the IAE criteria, outperforms these considered classical based methods in terms of settling time, overshoot and steady-state error indices. Indeed, the DC-link voltage performance using COA for designing the PI controller has a negligible steady-state error and also a negligible overshoot and it provides a shorter rise time than that in the case of a conventional adjustment method which presents a higher overshoot at the transient operation. For such reformulated PI design issues and in terms of offering the quality of solutions and non-premature convergence as well as fastness, the COA algorithm outperforms all other methods. To reinforce the effectiveness of the proposed COA method, the homologous PSO algorithm is considered for comparison purposes.

Figure 8 represents the dynamic response of the DC-link voltage based on the PI parameters design by COA and PSO. It can be observed from this figure, that COA can maintain the DC-link voltage to constant value faster than that of the other meta-heuristic (PSO). This confirms the higher global convergence of COA due to the impact of exploration and exploitation mechanisms that are developed by that algorithm. From Figure 8, the tracking dynamic indicates a considerable oscillating using the PSO algorithm for adjustment PI controller design and the COA tuned PI controller enables us to reach rapidly the steady-state. To confirm the reliability of COA compared to PSO, both algorithms executed 30 times. The population size and maximum of iterations are 20 and 50, respectively. The results of statistical comparison are presented in Table 3.
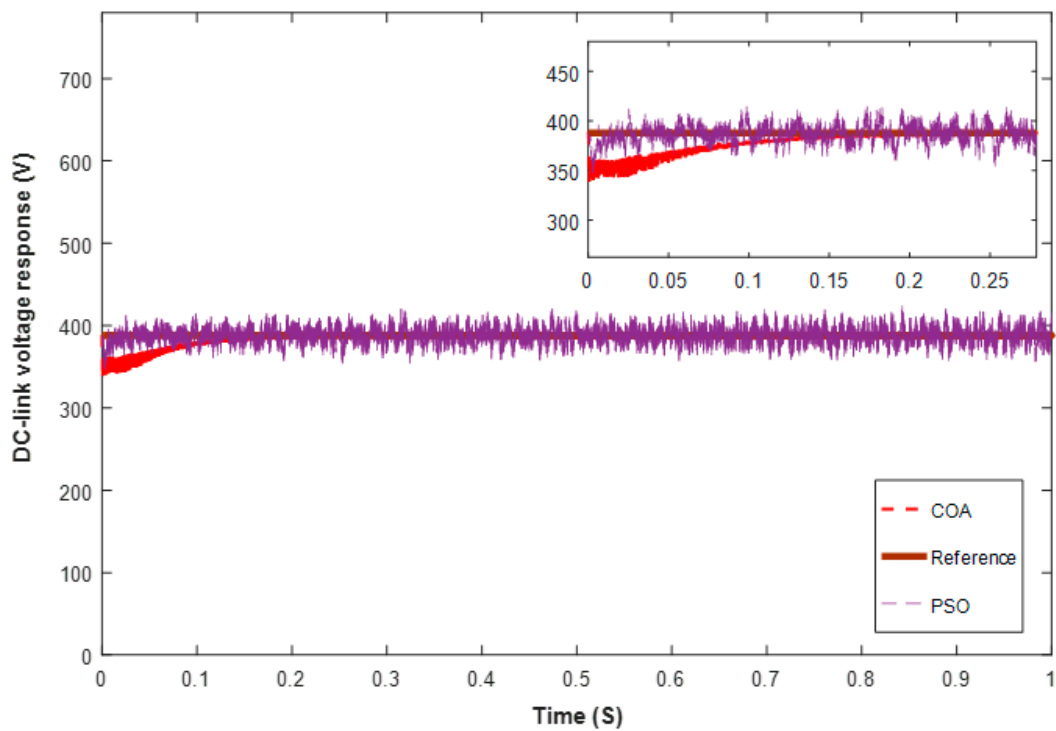
Figure 8. DC-link voltage responses using particle-swarm optimization (PSO) and COA.

Table 3. Statistical comparison between PSO and COA.

Algorithms	Best	Mean	Worst	Median	STD
PSO	3.4528	6.5660	9.8254	6.2777	2.23
COA	2.1696	5.3835	8.5281	5.8741	2.14

The detailed performance (power, speed, DC-link voltage, load torque, electromagnetic torque, etc. . . . .) of the PV generation system, obtained with COA algorithm used for tuning PI controllers design of the DC-link voltage and rotor speed, are illustrated in Figure 9.
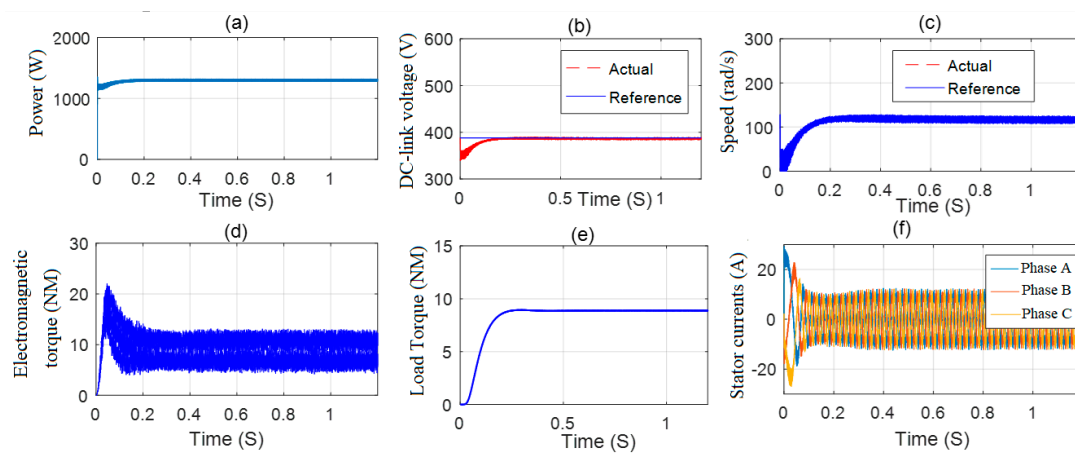

Figure 9. Performance of SPVWPS under partial shading condition using COA algorithm tuned PI controller of the DC link voltage and rotor speed. (**a**) power; (**b**) DC voltage; (**c**) speed; (**d**) electromagnetic torque; (**e**) load torque and (**f**) stator currents.

Considering Figure 9, it can be observed that the desired and the detected values of the rotor speed converge simultaneously to the nominal value that demonstrate the ameliorated efficiency of the speed control. Considering the heavy dependence between the rotor speed components and the load torque, the water spilling out of the pump was reduced due to sudden torque variation in the suggested regulation method. Figure 9c illustrates the rotor speed behavior of the PV system due to the increased proportionally of the load torque, however, it achieves steady-state shortly at 0.2 s.

However, the proposed system uses an MPPT algorithm that provides the reference speed as an output signal, to be fed into indirect-field oriented control (IFOC) strategy. It is worth noting that the reference and measured values of the DC bus voltage converge towards the desired value, which has demonstrated an enhanced efficiency of the voltage regulation. The reference value (set-point) of the DC bus voltage must be constant and its value was selected to 388 V. The outer PI controller loop is adopted to keep the DC bus voltage constant. The actual value of the DC bus voltage is the value that is measured by the voltage sensor.

In other words, this Set point (reference speed), which must be applied to the machine, comes from a new maximum power tracking algorithm based on the PSO technique (PSO-MPPT) and a pump affinity law (Equation (16)). This process results in an optimization of photovoltaic power under partial shading conditions. Further, it can be seen that the load torque and the rotor speed follow the PV power. This is found in Figure 9. It was found that the inaccuracy of the speed has an important effect on the efficiency and reliability of the pump drive (The relationship of proportionality was indicated in Equation (16)).

In sum, the COA algorithm can identify the gains of PI controllers of DC link voltage and rotor speed in a reduced computational time and under functional constraints compared to the reported classical techniques which usually provide local solutions for the control problem with constraints.

5. Conclusions

The optimal gains of PI controllers were determined using coyote optimization algorithm (COA) in order to enhance the effectiveness of the solar photovoltaic water-pumping system. In fact, the controllers' adjustment is reformulated as a constraint optimization problem under the functional time domain. A comparative study of the dynamic response of the DC-link voltage and rotor speed for the COA-tuning PI controllers is carried out with the well-known classical Ziegler–Nichols and Trial and Error tuning procedures. Similarly, the proposed meta-heuristic COA succeeds in the tune of PI controllers for DC-link voltage and rotor speed more effectively than the considered meta-heuristic PSO algorithm. The COA provides good responses of the DC-link voltage and rotor speed, during the transient and steady state cycle. The main outcomes confirmed the performance superiority of the developed COA-tuned PI controllers, in terms of the rapidity of convergence and solutions quality. To reduce the cost of the controller, a senseless-MPPT will be considered in the future work.

Author Contributions: Conceptualization, J.A., M.N.I. and H.R.; methodology, J.A., M.N.I and H.R.; software, J.A., H.R. and M.A.-D.; formal analysis, J.A., M.N.I., M.A. and H.R.; investigation, J.A., M.A.-D., M.A.; resources, J.A, M.A.-D. and H.R.; writing—original draft preparation, J.A., M.N.I., M.A.-D., M.A. and H.R.; writing—review and editing, J.A., M.N.I., M.A.-D., M.A. and H.R. All authors contributed equally to this work. All authors have read and agreed to the published version of the manuscript.

Conflicts of Interest: The authors declare no conflict of interest.Abbreviations

Abbreviations

ACO	Ant colony optimization
ANN	Artificial neural network
BA	Bat algorithm
COA	Coyote optimization algorithm
DC	Direct current

AC	Alternating current
DE	Differential evolution
DTC-SVM	Direct torque control–space vector modulation
GA	Genetic algorithm
GNFPID	Genetic neural fuzzy proportional integral derivative
GOA	Grasshopper optimization algorithm
GSC	Grid side converter
GWO	Gray wolf optimization
HSA	Harmony search algorithm
IAE	Integral absolute error
IFOC	Indirect field oriented control
MO	Maximum overshoot
MPP	Maximum power point
MPPT	Maximum power point tracking
PI	Proportional integral
PID	Proportional integral derivative
PSO	Particle-swarm optimization
PV	Photovoltaic
PWM	Pulse-width modulation
TIM	Three phase induction motor
RSC	Rotor side converter
SPVWPS	Solar photovoltaic water-pumping system
TEO	Thermal exchange optimization
VSI	Voltage source inverter
WCA	Water cycle algorithm

Symbols

f	Damping coefficient
I_{ds}, I_{qs}	Stator currents
L_m	magnetizing inductance
L_r	rotor inductance
P_n	Rated power
P_{pv}	PV power
T_e	Electromagnetic torque
T_r	Load torque
V_{dc}	DC-link voltage
V_{dr}, V_{qr}	Rotor voltages
V_{ds}, V_{qs}	Stator voltages
ω_m	Motor speed
ω_{mn}	Nominal value of mechanical speed
ω_{sl}	Sliding speed
φ_{dr}	Rotor flux
φ_{rn}	Nominal value of flux

References

1. Ibrahim, M.N.; Rezk, H.; Al-Dhaifallah, M.; Sergeant, P. Solar Array Fed Synchronous Reluctance Motor Driven Water Pump: An Improved Performance under Partial Shading Conditions. *IEEE Access* **2019**, *7*, 77100–77115. [CrossRef]

2. Ibrahim, M.N.; Rezk, H.; Al-Dahifallah, M.; Sergeant, P. Hybrid Photovoltaic-Thermoelectric Generator Powered Synchronous Reluctance Motor for Pumping Applications. *IEEE Access* **2019**, *7*, 146979–146988. [CrossRef]

3. Bouallègue, S.; Haggège, J.; Ayadi, M.; Benrejeb, M. PID-type fuzzy logic controller tuning based on particle swarm optimization. *Eng. Appl. Artif. Intell.* **2012**, *25*, 484–493. [CrossRef]

4.　Hu, H.; Hu, Q.; Lu, Z.; Xu, D. Optimal PID controller design in PMSM servo system via particle swarm optimization. In Proceedings of the 31st Annual Conference of IEEE Industrial Electronics Society, IECON 2005, Raleigh, India, 6–10 November 2005; pp. 79–83.

5.　Hasanien, H.M.; Muyeen, S.M. Design optimization of controller parameters used in variable speed wind energy Conversion system by genetic algorithms. *IEEE Trans. Sustain. Energy* **2012**, *3*, 200–208. [CrossRef]

6.　Ambia, M.N.; Hasanien, H.M.; Al-Durra, A.; Muyeen, S.M. Harmony search algorithm-based controller parameters optimization for a distributed-generation system. *IEEE Trans. Power Deliv.* **2015**, *30*, 246–255. [CrossRef]

7.　Blasko, V.; Kaura, V. A novel control to actively damp resonance in input LC filter of a three-phase voltage source converter. *IEEE Trans. Ind. Appl.* **1997**, *33*, 542–550. [CrossRef]

8.　Bingi, K.; Ibrahim, R.; Karsiti, M.N.; Chung, T.D.; Hassan, S.M. Optimal PID control of pH neutralization plant. In Proceedings of the 2nd IEEE International Symposium on Robotics and Manufacturing Automation, Ipoh, Malaysia, 25–27 September 2016; pp. 1–6.

9.　Mishra, K.P.; Kumar, V.; Rana, K.P.S. Stiction combating intelligent controller tuning: A comparative study. In Proceedings of the International Conference on Advances in Computer Engineering and Application, Ghaziabad, India, 19–20 March 2015; pp. 534–541.

10.　Ho, W.K.; Gan, O.P.; Tay, E.B.; Ang, E.L. Performance and gain and phase margins of well-known PID tuning formulas. *IEEE Trans. Control. Syst. Technol.* **1996**, *4*, 473–477. [CrossRef]

11.　Costa, B.L.G.; Graciola, C.L.; Angélico, B.A.; Goedtel, A.; Castoldi, M.F. Metaheuristics Optimization Applied to PI controllers Tuning of a DTC-SVM Drive for Three-Phase Induction Motors. *Appl. Soft Comput.* **2017**, *62*, 776–788. [CrossRef]

12.　Gizi, A.J.A.; Mustafa, M.; Jebur, H.H. A novel design of high-sensitive fuzzy pid controller. *Appl. Soft Comput.* **2014**, *24*, 794–805. [CrossRef]

13.　Zemmit, A.; Messalti, S.; Harrag, A. A new improved dtc of doubly fed induction machine using ga based pi controller. *Ain Shams Eng. J.* **2017**, *4*, 1–9. [CrossRef]

14.　Premkumar, K.; Manikandam, B. Speed control of brushless dc motor using bat algorithm optimized adaptive neuro-fuzzy inference system. *Appl. Soft Comput.* **2015**, *32*, 403–419. [CrossRef]

15.　Mohamed, M.A.; Diab, A.A.; Rezk, H. Partial shading mitigation of PV systems via different meta-heuristic techniques. *Renew. Energy* **2019**, *130*, 1159–1175. [CrossRef]

16.　Abdalla, O.; Rezk, H.; Ahmed, E.M. Wind driven optimization algorithm based global MPPT for PV system under non-uniform solar irradiance. *Sol. Energy* **2019**, *180*, 429–444. [CrossRef]

17.　Oshaba, A.S.; Ali, E.S. Speed control of induction motor fed from wind turbine via particle swarm optimization based pi controller. *Res. J. Appl. Sci. Eng. Technol.* **2013**, *5*, 4594–4606. [CrossRef]

18.　Douiri, M.R.; Cherkaoui, M. Neuro-genetic observer speed for direct torque neuro-fuzzy control of induction motor drive, Journal of circuits. *Syst. Comput.* **2012**, *21*, 1–18.

19.　Ali, E.S. Speed control of induction motor supplied by wind turbine via imperialist competitive algorithm. *Energy* **2015**, *89*, 593–600. [CrossRef]

20.　Rajasekar, N.; Sundaram, K.M. Feed-back controller design for variable voltage speed induction motor drive via ant colony optimization. *Appl. Soft Comput.* **2012**, *12*, 1566–1573. [CrossRef]

21.　Sundareswaran, K.; Nayak, P.S. Ant Colony based feedback controller design for soft-starter fed induction motor drive. *Appl. Soft Comput.* **2012**, *12*, 1566–1573. [CrossRef]

22.　Salvatore, N.; Caponio, A.; Neri, F.; Stasi, S.; Cascella, G.L. Optimization of delayed state kalman filter based algorithm via differential evolution for sensorless control of induction motors. *IEEE Trans. Ind. Electron.* **2010**, *57*, 385–394. [CrossRef]

23.　Costa, B.L.G.; Angélico, B.A.; Goedtel, A.; Castoldi, M.F.; Graciola, C.L. Differential evolution applied to dtc drive for three-phase induction motors using adaptive state observer. *J. Control Autom. Electr. Syst.* **2015**, *26*, 403–420. [CrossRef]

24.　Hato, M.M.; Bouallègue, S.; Ayadi, M. Water Cycle Algorithm-tuned PI Control pf a Doubly Fed Induction Generator for Wind Energy Conversion. In Proceedings of the 9th International Renewable Energy Congress (IREC), Hammamet, Tunisia, 20–22 March 2018; pp. 1–6.

25.　Hato, M.M.; Bouallègue, S. Direct Power Control Optimization for Doubly Fed Induction Generator Based Wind Turbine Systems. *Math. Comput. Appl.* **2019**, *24*, 77.

26. Arfaoui, J.; Rezk, H.; Al-Dhaifallah, M.; Elyes, F.; Abdelkader, M. Numerical Performance Evaluation of Solar Photovoltaic Water Pumping System under Partial Shading Condition using Modern Optimization. *Mathematics* **2019**, *7*, 1123. [CrossRef]

27. Devanshu, A.; Singh, M.; Kumar, N. DSP based feedback linearization control of vector controlled induction motor drive. In Proceedings of the 2016 IEEE 1st International Conference on Power Electronics, Intelligent Control and Energy Systems (ICPEICES), Delhi, India, 4–6 July 2016; pp. 1–6.

28. Hamid, K.H.A.N. *Field Oriented Control, Application Note*; Polytechech: Clermont-Ferrand, France, 2008.

29. Devanshu, A.; Singh, M.; Kumar, N. Sliding Mode Control of Induction Motor Drive Based on Feedback Linearization. *IETE J. Res.* **2020**, *66*, 256–269. [CrossRef]

30. Kim, S.-H. Maximum torque control of an induction machine in the field weakening region. *IEEE Trans. Ind. Appl.* **1995**, *31*, 787–794.

31. Singh, B.; Shukla, S.; Chandra, A.; Al-Haddad, K. Loss minimization of two stage solar powered speed sensorless vector controlled induction motor drive. In Proceedings of the IECON 2016—42nd Annual Conference of the IEEE Industrial Electronics Society, Florence, Italy, 24–27 October 2016; pp. 1–6.

32. Salim, D.; Kheldoun, A.; Sadouni, R. Fuzzy indirect field oriented control of dual star induction motor water pumping system fed by photovoltaic generator. *Int. J. Eng. Intell. Syst. Electr. Eng. Commun.* **2015**, *23*, 63–76.

33. Singh, S.; Singh, B. Solar PV water pumping system with DC-Link voltage regulation. *Int. J. Power Electr.* **2015**, *7*, 72–85. [CrossRef]

34. Wanzeller, A.M. Current control loop for tracking of maximum power point supplied for photovoltaic array. *IEEE Trans. Instrum. Meas.* **2004**, *53*, 1304–1310. [CrossRef]

35. Marouani, R.; Mami, A. Voltage Oriented Control Applied to a Grid Connected Photovoltaic System with Maximum Power Point Tracking Technique. *Am. J. Appl. Sci.* **2010**, *7*, 1168–1173. [CrossRef]

36. Consoli, A.R. Experimental low-chattering sliding-mode control of a pm motor drive. *Eur. Power Electr.* **1991**, *1*, 13–18.

37. Fathy, A.; Al-Dhaifallah, M.; Rezk, H. Recent Coyote Algorithm-Based Energy Management Strategy for Enhancing Fuel Economy of Hybrid FC/Battery/SC System. *IEEE Access* **2019**, *7*, 179409–179419. [CrossRef]

38. Pierezan, J.; Coelho, L.D.S. Coyote optimization Algorithm: A new metaheuristic for global optimization problems. In Proceedings of the 2018 IEEE Congress on Evolutionary Computation (CEC), Rio de Janeiro, Brazil, 29 January 2018; pp. 1–8.